Differential Cross-Section Measurements of Thin-Target Bremsstrahlung Produced by 2.7- to 9.7-Mev Electrons

N. STARFELT* AND H. W. KOCH
National Bureau of Standards, Washington, D. C.
(Received January 16, 1956)

The electron beam removed from a 50-Mev betatron and a total absorption scintillation spectrometer containing a sodium iodide crystal 5 in. in diameter and 9 in. long were used for the measurement of bremsstrahlung cross sections that are differential in photon energy and angle. Thin targets of beryllium, aluminum, and gold were bombarded by electrons with kinetic energies of 2.72, 4.54, and 9.66 Mev. The bremsstrahlung spectra from thick tungsten targets were also studied.

The results were compared with the differential cross-section predictions of Sauter, Schiff, and Gluckstern and Hull. The spectral shapes obtained with the beryllium and aluminum targets agreed with those expected from theory for the electron energies of 2.72 and 4.54 Mev. The 9.66-Mev experiment gave 20% more low-energy than intermediate-energy photons when compared with theory. For gold the experimental cross sections for the high photon energies are larger than theory with the differences increasing with decreasing electron primary energy. Evidence for electron-electron bremsstrahlung is obtained from the absolute magnitude of the differential cross sections, which are $(Z+1)/Z$ times larger than theory within the experimental errors. The thick-target tungsten spectra produced by 9.66-Mev electrons decreased more rapidly with increasing photon energy than did the thin-target cross sections derived by Schiff.

INTRODUCTION

SCATTERING of electrons in a nuclear Coulomb field results in a deceleration of the electrons and the production of x-rays, called bremsstrahlung. In the present experiment, the energies of individual x-ray photons were measured by a scintillation spectrometer in order to determine the absolute cross sections as well as the shapes of the angular and energy distribution of the x-rays. The results were compared with nuclear bremsstrahlung predictions for electrons with energies between 2.7 and 9.7 Mev.

At present, an exact bremsstrahlung theory exists only for very low incident electron energies. Sommerfeld[1] used the exact nonrelativistic wave functions for the electron and obtained a cross section which is differential in the x-ray energy and angle as well as in the scattered electron angle. Numerical integration of this cross section over the electron angle to obtain the cross section $d^2\sigma/d\Omega dk$, differential in photon energy and angle, was performed by Kirkpatrick and Wiedmann.[2]

Exact theories for incident electron energies of the order of, or greater than, the electron rest energy, m_0c^2, are complicated because the use of the exact Dirac wave functions necessary at these energies has not yet been successful. In addition, the screening of the nuclear field by the atomic electrons becomes important for high electron energies and materials of high atomic number and must be included in any theoretical calculations. Bethe and Maximon[3] have made an attempt at the use of Furry-Sommerfeld-Maue wave functions at extreme relativistic energies and provide an excellent review on the use of wave functions that are more exact than those assumed in the Born approximation.[4,5] However, the Bethe-Maximon formulas are not valid for primary energies less than about 20 Mev.[6]

Therefore, the only predictions of $d^2\sigma/d\Omega dk$ that are directly comparable with the present experiment are those obtained by means of the Born approximation. There are three such solutions available. Sauter[7] derived a cross section which gives the energy and angular distributions of bremsstrahlung, but without the screening correction. Gluckstern and Hull,[8] whose primary efforts were devoted to polarization calculations, also derived the Sauter formula with a crude correction for screening at low photon energies. Their results at other photon energies are not applicable when screening is important. Schiff[9] integrated the Bethe-Heitler differential cross section[4] over the outgoing electron angles in order to obtain a cross section that is differential in the photon energy and angle. He took the screening into account through the assumption of an atomic potential $(Ze/r)\exp(-r/a)$. However, the calculation is restricted to energies that are large compared to m_0c^2.

The general magnitudes of the errors to be expected in the theoretical bremsstrahlung predictions of the differential cross sections at energies larger than m_0c^2 can be inferred from the few experimental results.[10] For example, Curtis[11] at 60 Mev and Fisher[12] at 247 Mev found that their absolute cross sections near the upper

* On leave from the Radiation Physics Department, University of Lund, Lund, Sweden.

[1] A. Sommerfeld, Ann. Physik **11**, 257 (1931); *Atombau und Spektrallinien* (Friedrich Vieweg und Sohn, Braunschweig, 1939).

[2] P. Kirkpatrick and L. Wiedmann, Phys. Rev. **67**, 321 (1945).

[3] H. A. Bethe and L. C. Maximon, Phys. Rev. **93**, 768 (1954).

[4] H. A. Bethe and W. Heitler, Proc. Roy. Soc. (London) **A146**, 83 (1934).

[5] W. Heitler, *The Quantum Theory of Radiation* (Oxford University Press, New York, 1954).

[6] See also the comments of H. Olsen, Phys. Rev. **99**, 1335 (1955).

[7] F. Sauter, Ann. Physik. **20**, 404 (1934).

[8] R. L. Gluckstern and M. H. Hull, Phys. Rev. **90**, 1030 (1953).

[9] L. I. Schiff, Phys. Rev. **83**, 252 (1951).

[10] D. R. Corson and A. O. Hanson, Ann. Rev. Nuc. Sci. **3**, 67 (1953).

[11] C. D. Curtis, Phys. Rev. **89**, 123 (1953).

[12] P. C. Fisher, Phys. Rev. **92**, 420 (1953).

part of the x-ray spectrum were 7 and 8.7%, respectively, below the Bethe-Heitler predictions. Hagerman and Crowe[13] in a similar experiment at 500 Mev agreed with theory to within the combined experimental errors of 25%. The relative shapes of the x-ray spectra that have been measured show reasonable agreement with theory in the range from 10 to 500 Mev.[14–21] The more extensive measurements of the spectral and angular distribution of bremsstrahlung at 0.5 and 1 Mev by Motz[22] were made with a large-crystal sodium iodide scintillation spectrometer and thin targets. His cross sections were larger than the Born approximation cross sections[7] in this energy region. The exact bremsstrahlung calculations of Jaeger[23] for lead, which were done numerically for an electron total energy, E_0, of 1.53 Mev confirm the general results found by Motz. Jaeger found that the results of his exact, but limited, calculations were larger than the Born approximation values of 31% at a photon energy, k, of 0.76 Mev and by 350% at a photon energy of 0.99 Mev.

These results[11–23] show that the bremsstrahlung cross-section values are larger than theory at low incident electron energies and smaller than theory at high energies. Pair production cross sections when compared to theory show the same trend with a definite cross-over at about 5 Mev.[10] Therefore, the electron energy range from 2.7 to 9.7 Mev selected for study in this experiment might encompass a transition region for bremsstrahlung. This range should also help to bridge the gap between the energy of 1 Mev at which Motz[22] obtained detailed data and the energy band from 10 to 30 Mev in which detailed spectra for the interpretation of photodisintegration experiments are needed and lacking.

EXPERIMENTAL ARRANGEMENT

The experimental arrangement for the measurement of the bremsstrahlung cross sections is shown in Fig. 1. The electron beam in the National Bureau of Standards 50-Mev betatron was expanded and extracted from the acceleration tube by means of an electromagnetic extractor.[24] The electron pulse thus obtained had an approximate duration of 0.1 microsecond at a repetition rate of 180 pulses per second.

The beam was passed through a plastic foil 2 mg/cm² thick into a system of three Lucite collimators in order to make the angular aperture of the beam small (0.80°) compared to the half-intensity angle of the bremsstrahlung angular distribution to be studied. The Lucite collimators were succeeded by lead collimators, the holes of which were made large enough so that the electron beam would not strike the lead.

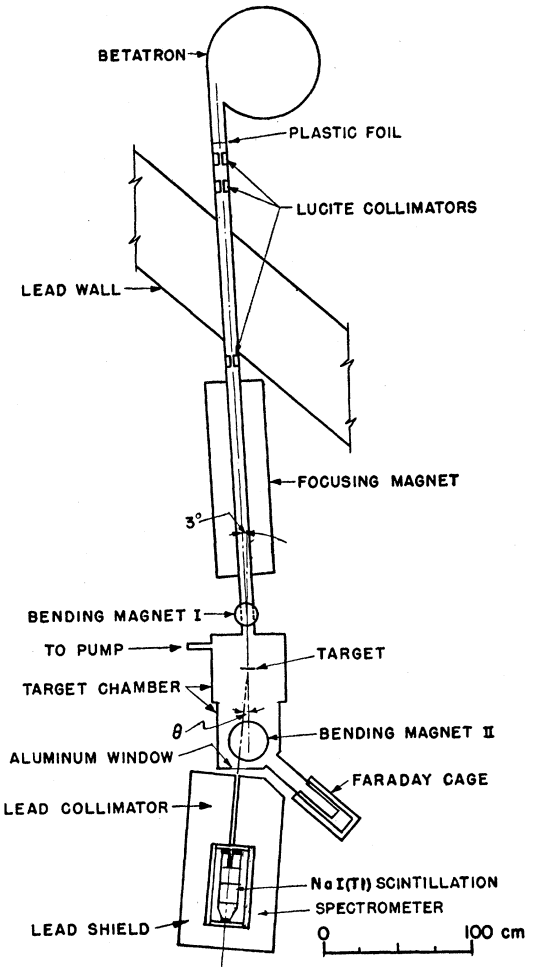

FIG. 1. Experimental arrangement for the measurement of bremsstrahlung spectra.

After passing through the collimator system, the beam was focused on the bremsstrahlung target by an iron-cored magnetic lens. In order to suppress the background counts produced by radiation from the betatron and the collimator system, the beam was bent 3° around a vertical axis by means of a small electromagnet before the electrons struck the target. The target chamber consisted of a cubic aluminum box 50 cm on a side. The targets were mounted on aluminum rings 1 mm thick with 52 mm inside diameters. These rings were supported by aluminum rods, 196 mm long and 3 mm in diameter, mounted on a table that could be rotated from the outside of the box. Thus, it was possible to have four targets inside the box and place any one of them in the beam.

[13] D. C. Hagerman and K. M. Crowe, Phys. Rev. **100**, 869 (1955).
[14] Motz, Miller, and Wyckoff, Phys. Rev. **89**, 968 (1953).
[15] H. W. Koch and R. E. Carter, Phys. Rev. **77**, 165 (1950).
[16] V. E. Krohn and E. F. Shrader, Phys. Rev. **87**, 685 (1955).
[17] E. V. Weinstock and J. Halpern, Phys. Rev. **100**, 1293 (1955).
[18] R. H. Stokes, Phys. Rev. **84**, 991 (1951).
[19] J. W. DeWire and L. A. Beach, Phys. Rev. **83**, 476 (1950).
[20] Powell, Hartsough, and Hill, Phys. Rev. **81**, 213 (1951).
[21] D. H. Cooper, California Institute of Technology, thesis, 1955 (unpublished); Leiss, Hanson, and Yamagata, University of Illinois Report, 1954 (unpublished).
[22] J. W. Motz, Phys. Rev. **100**, 1560 (1955).
[23] J. C. Jaeger, Nature **140**, 108 (1937).
[24] R. S. Foote and B. Petree, Rev. Sci. Instr. **25**, 694 (1954).

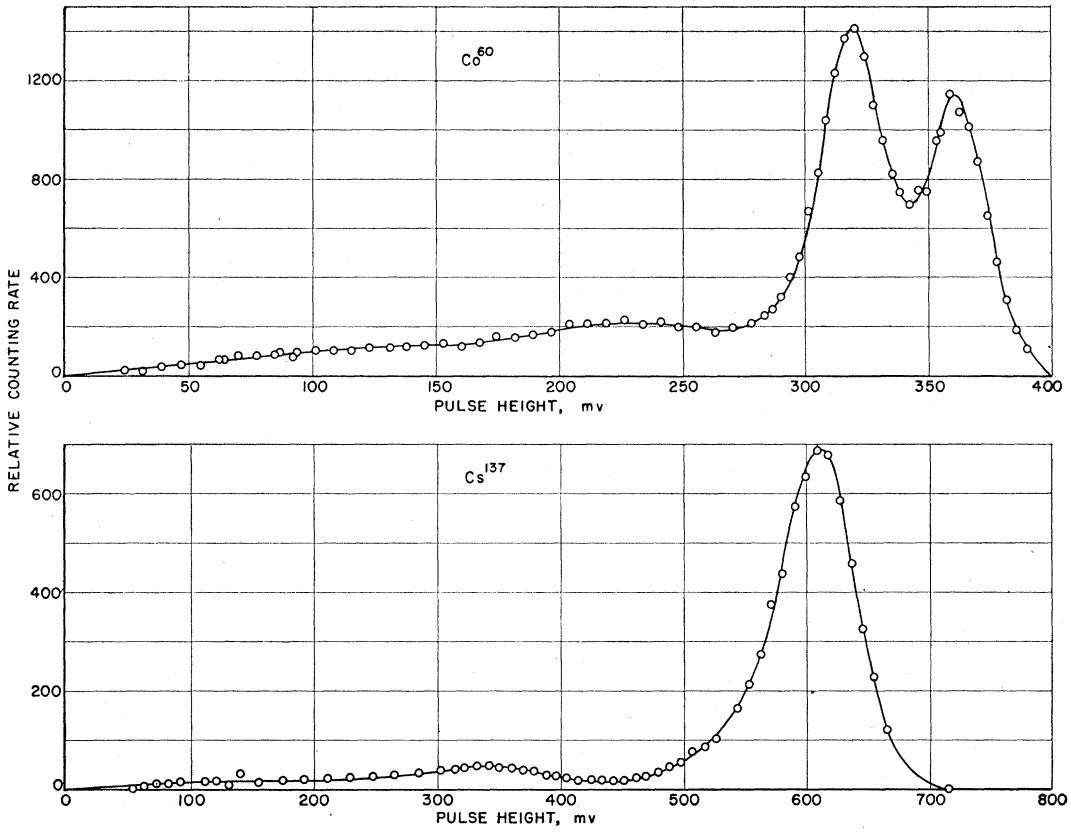

FIG. 2. Pulse-height distributions produced by the 0.66-Mev gamma rays from Cs^{137} and the 1.17- and 1.33-Mev gamma rays from Co^{60} in a NaI(Tl) scintillation spectrometer 5 in. in diameter and 9 in. long. The sources were located at the target position in the experimental arrangement of Fig. 1.

The beam, having passed through the thin target, passed out into an extension of the aluminum box, which was in the vertical field of an electromagnet having pole faces of 24 cm diameter. Here the beam was bent 45° and passed into an aluminum tube which ended in a Faraday cage consisting of an aluminum cylinder supported by Lucite insulators. The walls and bottom of the cage were 1.5 cm and 7.5 cm thick, respectively. The type of Faraday cage was previously studied by Laughlin.[25] His experience and that of Berman and Brown[26] showed that the loss of charge caused by bremsstrahlung is negligible in the energy range of interest. The vacuum system consisting of the Faraday cage, target chamber, and collimator tube was kept at a vacuum better than 10^{-4} mm Hg by an oil diffusion pump. The electrons caught by the Faraday cage were collected on a condenser and the voltage of this condenser was measured with a calibrated vibrating reed electrometer. After small corrections were made for leakage currents, which were measured daily, the condenser voltage gave the absolute electron charge. These measurements showed that the electron currents were of the order of 10^{-11} ampere. A NaI(Tl) scintillation counter was mounted at the back of the Faraday cage in order to give a continuous indication of the beam intensity. The output from the counter was fed into a chart recorder.

The bremsstrahlung emitted from the target left the vacuum through an aluminum window 0.035 mm thick, passed through a cadmium filter 0.81 mm thick and a lead collimator, which was pointed at the target, and was finally absorbed by the NaI(Tl) crystals of the total absorption spectrometer. The aperture of the collimator was a hole 1.5 cm in diameter in a total lead thickness of 46 cm. The end of the collimator hole subtended an angle of 0.7° at the target.

The collimator-spectrometer system was mounted on a rigid table which could be rotated around a vertical axis through the target. The range of rotation was from 4° on one side of the direction of the electron beam to 12° on the other side. The angle was measured by means of a precision scale at the back of the table.

The total absorption scintillation spectrometer consisted of two NaI(Tl) crystals together forming a cylinder of 5-in. diameter and 9-in. length.[27] The light from the front crystal was detected by four DuMont

[25] J. S. Laughlin (private communication).
[26] A. I. Berman and K. L. Brown, Phys. Rev. **86**, 83 (1954).
[27] R. S. Foote and H. W. Koch, Rev. Sci. Instr. **25**, 746 (1954).

6292 photomultipliers separated from the flat circular surface of the crystal by a glass plate. The beam entered the crystal at the center of the surface where the glass had been made thin and was not covered by the photomultipliers. The light from the back crystal was detected by a DuMont 6364 photomultiplier 5 in. in diameter. The spectrometer system was shielded by at least 20 cm of lead on all sides.

The pulses from the photomultipliers were added and amplified in a Chase-Higinbotham nonoverloading amplifier[28] and a post-amplifier giving an extra gain of three. The amplified pulses were analyzed in three ten-channel pulse-height analyzers (Los Alamos model No. 103) which were gated on for 15 microseconds by a pulse from the betatron expansion circuit.

EXPERIMENTAL PROCEDURE

The alignment of the electron beam collimating system and the focusing magnet was accomplished by photographic films that detected the electron beam at various parts of the vacuum system. Thus, it was shown that the diameter of the focal spot at the target holder position was less than 6 mm for all the energies used. The collimator and spectrometer were accurately aligned with the focal spot by the aid of a zirconium-arc source which projected the images of temporary cross hairs, located on the target holder and at the back aluminum window position, on to the spectrometer.

The response of the scintillation spectrometer to a single gamma-ray line was involved in the evaluation of the photon spectrum from the measured pulse-height distribution. To determine the response experimentally at two gamma-ray energies, an evaporated Cs^{137} and a calibrated Co^{60} source were placed at the center of the target holder and the pulse-height distributions obtained from the spectrometer were recorded (Fig. 2). The Co^{60} source used was absolutely calibrated[29] and the total counting rate of this source thus provided a means of measuring the spectrometer total efficiency for a radiation source at the target position. The measured counting rate gave an efficiency 3% lower than the calculated efficiency. Another test of the gamma-ray measurements was obtained from a comparison of the photofraction, p^*, obtained from Fig. 2 and from the Monte Carlo calculations of Berger and Doggett.[30] The quantity p^* is defined as the ratio of the area under the "photopeak" of the pulse-height distribution to the area under the entire pulse-height distribution. At 0.662, 1.17, and 1.33 Mev the values of p^*, according to Berger and Doggett, for the present spectrometer were 0.89, 0.78, and 0.77, respectively, which are 5% greater than the p^* calculated from the distributions for Cs^{137} and Co^{60} in Fig. 2. The experimental errors due to background and scattering in the collimator were estimated to be of this same order of magnitude.

The spectra from 2.63-mg/cm² Be, 0.878-mg/cm² Al, and 0.209-mg/cm² Au targets were measured for electron kinetic energies of 2.72 Mev, 4.54 Mev, and 9.66 Mev at angles between the direction of the incoming electron beam and the axis of the scintillation spectrometer ranging from 0° to 6°. The target thicknesses corresponded to electron energy losses of 6 kev for Be, 2 kev for Al, and 0.6 kev for Au. Furthermore, the radiation from three thick W targets (240 mg/cm², 489 mg/cm², 5800 mg/cm²) was studied at 4.54 and 9.66 Mev at 0° and 12°.

The direction of the electron mean was determined by a measurement of the angular distribution of the total number of bremsstrahlung photons above a certain energy. Measurements were taken with the spectrometer on both sides of the electron beam as shown in the angular distribution for beryllium in Fig. 3. The 0° direction of the photons was determined with an accuracy of ±0.2°.

Each spectrum consisted of 40 000 to 50 000 counts divided into 40 pulse-height analyzer channels. To get a better measurement of the absolute bremsstrahlung cross section, the integrated number of counts in these different spectra was measured several times. Examples of two of the experimental spectra are given in Fig. 4. Also shown on this figure are the background counts obtained with no target in the electron beam. This background was measured separately for each combination of electron energy and photon angle and was analyzed into no-beam and beam background.

The energy of the bremsstrahlung photons was determined by comparison with the 1.11-Mev gamma-ray

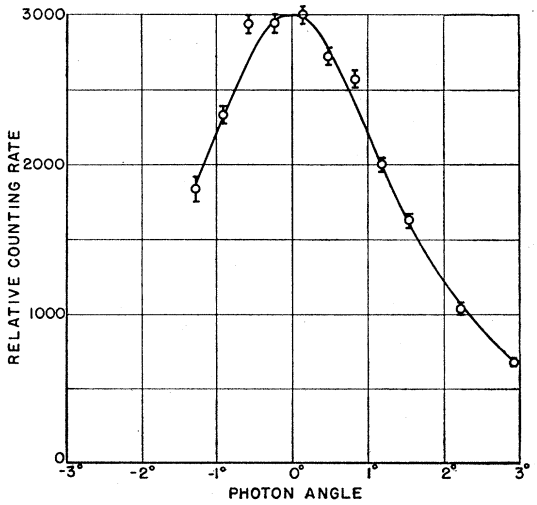

FIG. 3. The angular distribution of the total number of photons above 0.5 Mev for a 2.63-mg/cm² Be radiator and 9.66-Mev primary electron kinetic energy.

[28] R. L. Chase and W. A. Higinbotham, Rev. Sci. Instr. **23**, 34 (1952).

[29] The calibration was performed by G. Minton who used a coincidence measurement of the Co^{60} source activity. A report on this work is in preparation.

[30] M. Berger and J. Doggett, J. Research Natl. Bur. Standards (to be published).

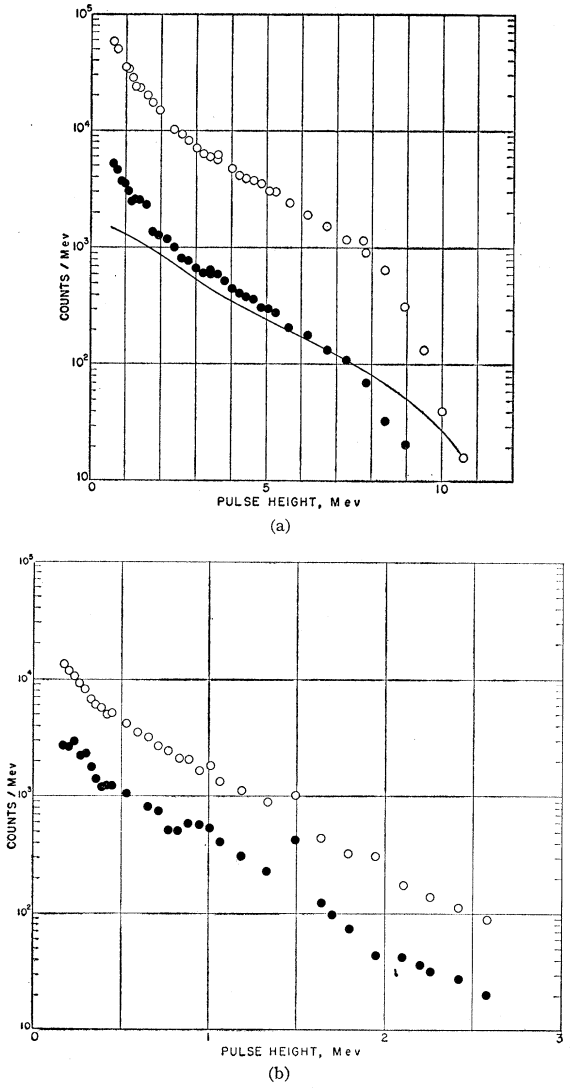

FIG. 4. Experimental pulse-height distributions (open circles), and background pulse-height distributions (filled circles) for (a) Be, 9.66 Mev, 0° (an example of relatively low background) and for (b) Au, 2.72 Mev, 0° (an example of relatively large background). The solid line in (a) is the double pulse spectrum, which was negligible for the 2.72-Mev case in (b).

line from Zn^{65}. For this purpose the pulse-height distribution of this line was measured at least twice a day, with a Zn^{65} source in front of the lead collimator. The position of this peak was determined in terms of the height of the pulse from a mercury switch precision pulser connected to the input of the nonoverloading amplifier. Pulses from this pulser were then used to determine the boundaries of each 10-channel pulse-height analyzer. This energy calibration was stable to $\pm 0.5\%$ over a period of 24 hours. The width of the pulse-height analyzer windows were measured, with the above mentioned precision pulser used as a sliding pulser. This window width varied less than $\pm 3\%$ during 24 hours.

In order to measure the energy of the electrons in the beam, one of the spectrometer crystals was placed close to the aluminum window (Fig. 1), and the electron beam was focused on the crystal. Voltage pulse-height distributions shown in Fig. 5 were produced by the individual detection of electrons. The position of the peaks of these distributions were compared with those obtained with the gamma rays from Co^{60}. To obtain the energy of the electrons, a correction for the energy loss in the aluminum container and the magnesium oxide surrounding the crystal was made. Because the amount of MgO was unknown, the total amount of matter intercepting the electron beam was measured by means of the absorption of the 22-kev x-ray line from a Cd^{109} source. The most probable energy loss of the electrons was calculated to be 300 kev. The electron kinetic energies measured in this manner were 2.72, 4.54, and 9.66 Mev for the three different operating energies of the betatron that were used. These energies were estimated to be constant and known with a probable error of less than $\pm 0.5\%$.

The measurement of the thickness of the targets was of primary importance in the determination of absolute cross sections. This thickness was chosen small enough to make the average scattering angle of electrons small compared to the full width at half-intensity of the angular distribution of the bremsstrahlung. That this was the case was proved by measuring the angular distribution using two targets the thicknesses of which differed by about a factor of two. Both targets gave the same angular distribution. This should be a sensitive check because in the case of appreciable multiple scattering the angular distribution would be broadened. The thinnest of the two targets was used in the final experimental determinations.

The average thickness of a target was determined by weighing. The uniformity of the foils was studied by measuring the transmission of beta rays from a S^{35} source through different parts of the foil. The Be foil used appeared to be uniform to $\pm 1.5\%$. The Al target which consisted of four superimposed foils unfortunately showed variations of as much as $\pm 5\%$ within the area of interest. The Au target was still more nonuniform. Therefore, in the case of gold, the total number

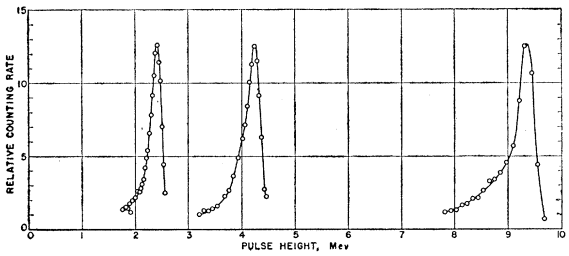

FIG. 5. Pulse-height distributions produced by individual electrons in a scintillation spectrometer containing a NaI(Tl) crystal 5-in. in diameter and 4 in. long. The electron kinetic energies inferred from these peaks after correction for the energy loss in the spectrometer window were 2.72, 4.54, and 9.66 Mev.

of counts above a certain pulse-height level was measured using twenty different points on the same foil as targets. The average counting rate thus obtained was used to normalize the measured spectral distribution. The error in the absolute cross section was decreased by this method to $\pm 2\%$.

The chemical purity of the Be target is of great importance because of the low atomic number. Therefore, the target used in the experiment was spectrochemically analyzed.[31] It was found to contain 8.0% O, 0.14% Cr, 0.14% Fe, and 0.25% Si. Almost all of the oxygen was found in a layer of BeO on the surface of the Be foil.

EVALUATION OF THE BREMSSTRAHLUNG SPECTRUM FROM THE MEASURED PULSE-HEIGHT DISTRIBUTION

A number of corrections had to be applied in order to convert the measured pulse-height distributions into differential cross sections. The most important of these corrections took into account the following effects: (1) pileup of counts, (2) background counting rate, (3) response of the spectrometer to different photon energies, (4) absorption of photons between target and spectrometer, and (5) collimator effects.

(1) The short duration of the betatron burst (approximately 0.1 microsecond) compared to the length of the delay-line shaped pulse entering the pulse-height analyzer (approximately 1 microsecond) made the calculation of the spectrum of double pulses possible, because the height of a double pulse was simply the sum $(\epsilon_1+\epsilon_2)$ of the two single pulses. Therefore, the spectrum of double pulses is given by

$$P''(\epsilon)=p\frac{\int_0^{\epsilon} P(\epsilon_1)P(\epsilon-\epsilon_1)d\epsilon_1}{\int_0^{\epsilon_{\max}} P(\epsilon_1)d\epsilon_1}, \quad (1)$$

where $P(\epsilon_1)$ is a spectrum of single pulses and p is the ratio of the probability during a spectrum experiment of recording two photons in the same burst in the spectrometer to the probability for recording only one photon. p was obtained from the expression $p=\sum x^2/2\sum x$, where x was the average number of spectrometer pulses per betatron burst as inferred from the current record from the Faraday cage scintillation counter and the sum is performed over all betatron pulses. $P''(\epsilon)$ can be calculated by successive approximations by using the measured spectrum as a first approximation for $P(\epsilon_1)$. In the present case, the first approximation was shown to give sufficient accuracy.

The pulse spectrum $P''(\epsilon)$ was subtracted from the measured pulse-height distribution and the remaining spectrum was multiplied by $(1+2p)$ to correct for the loss of single pulses through the pileup. Since p was kept below 5% throughout the experiment, the pile-up correction was important only for photon energies close to the upper end of the spectrum, as can be seen from Fig. 4(a).

(2) The next step was to subtract the background counts. Fortunately most of the background was bremsstrahlung and so the background spectrum had approximately the same shape as the spectra to be studied. Figure 4 shows the background correction for two different spectra. The relative background varied from 10 to 30% of the total counts measured and was largest for the lowest electron energy of 2.72 Mev. The background correction was approximately the same for Be, Al, and Au and much less for W at a given energy.

(3) If the spectrum of the photons incident on the spectrometer is $N(k)dk$, where k is the photon energy, the pulse height distribution $P(\epsilon)d\epsilon$ obtained from the crystal photomultiplier system is given by

$$P(\epsilon)d\epsilon=d\epsilon\int_0^{k_{\max}} K(k,\epsilon)N(k)[1-e^{-\mu L}]dk, \quad (2)$$

where μ is the total absorption coefficient of NaI at the energy k, L is the length of the crystal, $k_{\max}$ the maximum energy in the spectrum, and $K(k,\epsilon)$, the response function of the crystal to a single gamma-ray line of the energy k, i.e., the pulse-height distribution produced in the spectrometer by the gamma-ray line.

$P(\epsilon)$ being the measured pulse-height distribution, Eq. (2) above had to be solved with respect to $N(k)$. This can be accomplished in different ways.[22,32] In the present investigation Eq. (2) was transformed into a matrix form.

Integration over the interval $\Delta\epsilon_j$ of the variable ϵ and replacement of the integral over k in Eq. (2) by a sum of integrals over intervals Δk_i, gives

$$\int_{\epsilon_j-\frac{1}{2}\Delta\epsilon_j}^{\epsilon_j+\frac{1}{2}\Delta\epsilon_j} P(\epsilon)d\epsilon=\int_{\epsilon_j-\frac{1}{2}\Delta\epsilon_j}^{\epsilon_j+\frac{1}{2}\Delta\epsilon_j} d\epsilon\sum_{i=0}^{n}\int_{k_i-\frac{1}{2}\Delta k_i}^{k_i+\frac{1}{2}\Delta k_i} K(k,\epsilon)\times N(k)[1-e^{-\mu L}]dk. \quad (3)$$

On the assumption that $P(\epsilon)$ and $N(k)$ vary only slowly within an interval, Eq. (3) can be written

$$\langle P(\epsilon)\rangle_j\Delta\epsilon_j=\sum_{i=0}^{n}\langle N(k)\rangle_i\int_{\Delta\epsilon_j} d\epsilon\int_{\Delta k_i} K(k,\epsilon)[1-e^{-\mu L}]dk. \quad (4)$$

The angular braces $\langle\ \rangle$ denote the average value of the function in the interval under consideration. $\langle P(\epsilon)\rangle$ and $\langle N(k)\rangle$ can be represented as matrices, and Eq. (4) representing a set of simultaneous equations can be rewritten as

$$\langle P(\epsilon)\rangle=M\langle N(k)\rangle, \quad (5)$$

[31] Spectrochemical analysis by B. F. Scribner, National Bureau of Standards; thickness of oxygen layer determined by J. Stonehouse, The Brush Beryllium Company.

[32] K. Liden and N. Starfelt, Arkiv Fysik 7, 427 (1954).

TABLE I. The significant elements of the 15th, 35th, and 55th rows of the transpose of the 56×56 response matrix, M_{ji}, and of the inverse matrix, M_{ji}^{-1}. k_i and ϵ_j are the photon energy and pulse height corresponding to the midpoint of the respective intervals.

$i=15$	j	11	12	13	14	15	16	17	18	19	20	21	22
	ϵ_j Mev	0.353	0.423	0.499	0.582	0.671	0.767	0.869	0.978	1.092	1.214	1.341	1.475
$k_i=0.671$ Mev	$100\times M_{ji}'$	1.8	3.2	1.8	11.9	64.7	11.8	0.0	0.0	0.0	0.0	0.0	0.0
	$100\times M_{ji}^{-1}$	0.2	−1.1	6.0	−31.5	165.9	−30.5	2.0	−7.0	−3.8	−3.9	−2.0	1.3
$i=35$	j	31	32	33	34	35	36	37	38	39	40	41	42
	ϵ_j Mev	2.967	3.165	3.369	3.580	3.796	4.020	4.250	4.485	4.727	4.976	5.231	5.493
$k_i=3.796$ Mev	$100\times M_{ji}'$	2.6	7.0	10.3	11.2	44.0	8.0	0.0	0.0	0.0	0.0	0.0	0.0
	$100\times M_{ji}^{-1}$	0.3	−1.7	8.8	−46.4	245.4	−43.6	−53.0	−1.5	13.7	−2.2	−5.9	0.2
$i=55$	j	51	52	53	54	55	56						
	ϵ_j Mev	8.133	8.458	8.790	9.128	9.472	9.823						
$k_i=9.472$ Mev	$100\times M_{ji}'$	2.8	3.9	12.6	20.0	32.0	5.6						
	$100\times M_{ji}^{-1}$	0.5	−2.9	14.8	−76.3	394.3	−230.3						

where the elements of the square matrix M are given by

$$M_{ji}=\int_{\Delta\epsilon_j} d\epsilon \int_{\Delta k_i} K(k,\epsilon)[1-e^{-\mu L}]dk \Big/ \Delta\epsilon_j. \quad (6)$$

The matrix used in the present calculation was composed of 56 rows and 56 columns and covered the energy region 0 to 10 Mev. Because the half-intensity width of the photopeak of a single gamma-ray line is proportional to $\sqrt{k}$ the intervals Δk and $\Delta\epsilon$ were chosen to be proportional to $\sqrt{k}$ and $\sqrt{\epsilon}$ respectively. The matrix elements M_{ji} were obtained by numerical integration of $K(k,\epsilon)$ in the regions where this function varied fast with k or ϵ. In the case of slow variation of $K(k,\epsilon)$, M_{ji} was calculated as

$$M_{ji}=K(k_i,\epsilon_j)[1-e^{-\mu_i L}]\Delta k_i. \quad (7)$$

The function K was calculated by Berger and Doggett[30] for energies up to 4.45 Mev using the Monte Carlo method. Above 4.45 Mev there exist no detailed calculations and no suitable single gamma-ray lines that can be used for the determination of K. However, at $k=11$ Mev, Koch and Wyckoff[33] determined K by a synthesis procedure based on experimental data obtained with monoenergetic electrons. Therefore, at k equal to 5 and 8 Mev, K was calculated by a combination of the Berger and Doggett data and the Koch and Wyckoff procedure.

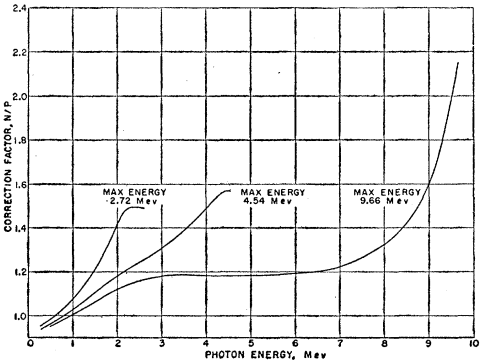

FIG. 6. The correction factor N/P calculated for bremsstrahlung spectra with maximum photon energies of 2.72, 4.54, and 9.66 Mev, respectively.

[33] H. W. Koch and J. Wyckoff, J. Research Natl. Bur. Standards (to be published).

In order to obtain the photon distribution, $N(k)$, from Eq. (5), the matrix M was first inverted by the National Bureau of Standards automatic computer, the SEAC. Examples of elements of the transpose of the matrix, M_{ji}, and the inverse, M_{ji}^{-1}, are given in Table I. The elements of the transpose are given in order to show the shape of a pulse-height distribution due to a monoenergetic gamma ray. The function $P(\epsilon)$ obtained by fitting a smooth curve to the measured points of a pulse-height distribution was then multiplied by M^{-1} in the SEAC in order to give $N(k)$. After this procedure had been tried for a number of test spectra, it became apparent that the correction factor $N(k)/P(\epsilon)$ was almost the same for the extremes of the spectral shapes obtained in this experiment for a given electron energy. Therefore, curves of the correction factor as given in Fig. 6 were used to convert individual points on $P(\epsilon)$ into points in $N(k)$.

(4) To obtain the bremsstrahlung spectrum emitted from the target, the spectrum obtained above was corrected for the absorption in the Cd filter and the glass window of the spectrometer.

In calculating the solid angle of the spectrometer as seen from the target, a correction for transmission of photons through the walls of the collimator had to be applied. The fractional increase, A, of the solid angle due to this process is given by

$$A=\frac{2\pi l^2}{S}\int_{\phi_1}^{\phi_2} e^{-\mu x}\sin\phi d\phi, \quad (8)$$

where l is the distance between the target and the spectrometer end of the collimator, $x=(1/\cos\phi)-(r/\sin\phi)$, S the area and r the radius of the hole in the collimator, μ the total absorption coefficient of the collimator material, and ϕ the angle between the photon direction and the center line through the target and the collimator. Taking into account that $e^{-\mu x}$ decreases very rapidly with increasing ϕ, the fraction A can be shown to be given by $A=2/\mu l$, which was less than 3.5% for all energies in the present experiment.

Furthermore, the scattering into the crystal of photons striking the walls of the collimator was estimated. An approximate calculation of this effect con-

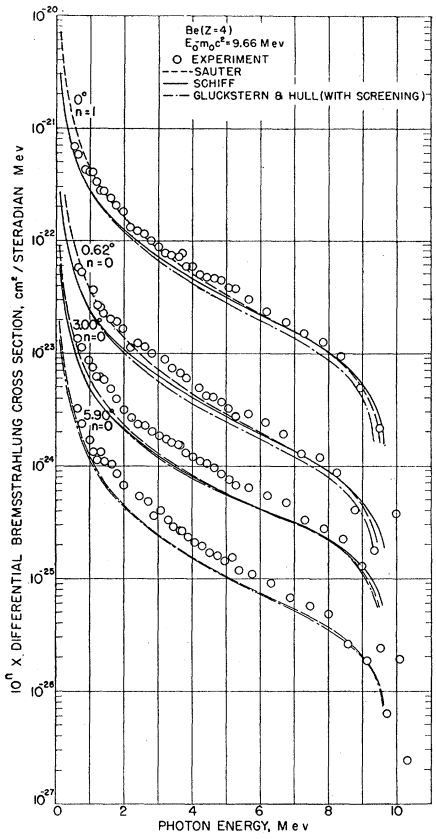

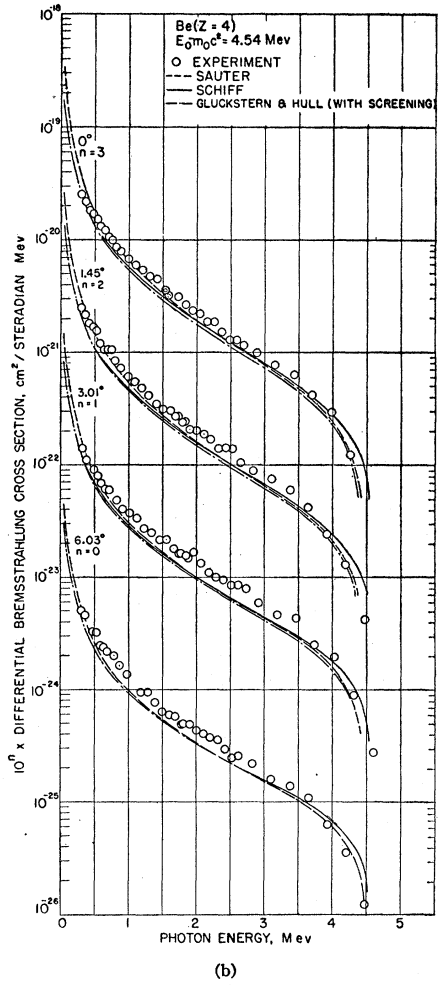

FIG. 7. Corrected experimental differential cross sections $d^2\sigma/d\Omega dk$ and theoretical cross sections according to Sauter, Gluckstern and Hull, and Schiff, respectively, for Be($Z=4$) and for electron kinetic energies of (a) 9.66 Mev, (b) 4.54 Mev, and (c) 2.72 Mev.

sidering single scattering only shows that the contribution of scattered photons for the measured spectra is less than 1.5% at all energies. Because of the uncertainty of the calculation and the small magnitude, this correction was neglected.

The measurement of the counting rate from an absolutely calibrated Co^{60} source located at the target position gave a very good confirmation of the calculations of the solid angle of the spectrometer, the transmission of photons through the collimator material and the scattering of photons in the collimator for an energy of about 1.2 Mev. Therefore, the procedure outlined was used to correct for collimator effects at all energies.

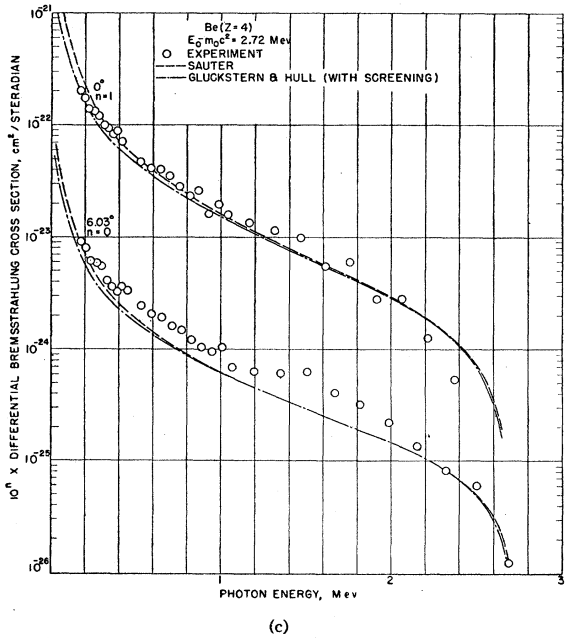

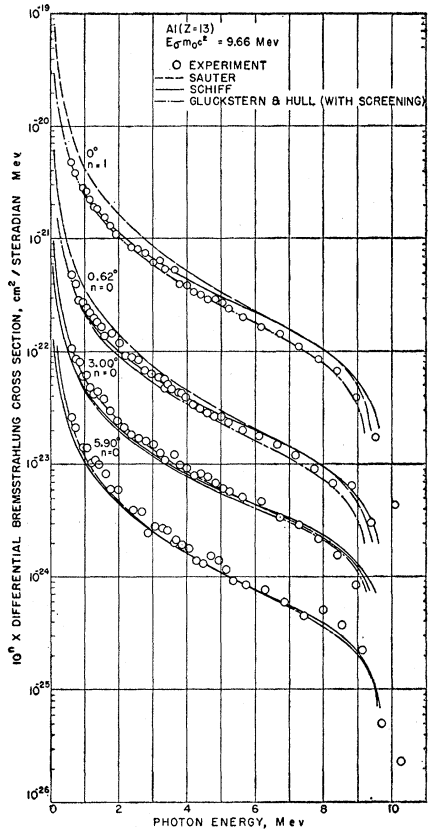

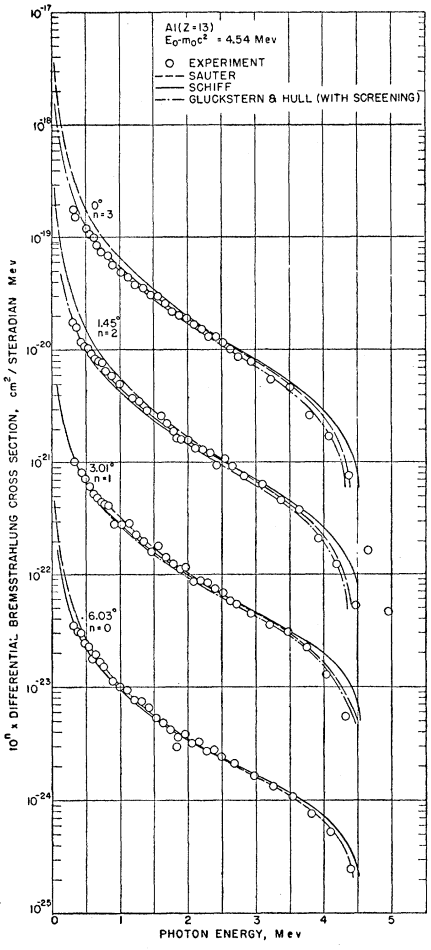

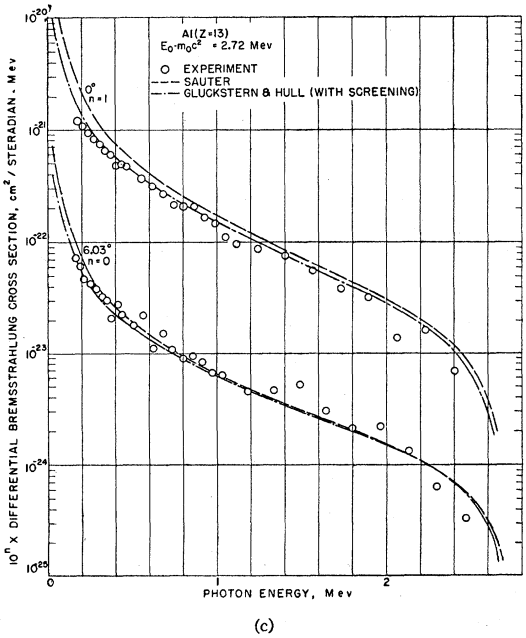

FIG. 8. Corrected experimental cross sections $d^2\sigma/d\Omega dk$ and theoretical cross sections according to Sauter, Gluckstern and Hull, and Schiff, respectively, for Al($Z=13$) and for electron kinetic energies (a) 9.66 Mev, (b) 4.54 Mev, and (c) 2.72 Mev.

THIN-TARGET RESULTS

The experimental results are shown in Figs. 7–9 as semilogarithmic plots of the differential cross section *versus* photon energy. The logarithmic scale was necessary in order to allow the experimental and theoretical curves for all the angles to be plotted on the same graphs. An example of the data for two cases, transformed into curves of intensity, $k(d^2\sigma)/(d\Omega dk)$, is given in Fig. 10. Analyses of these data will be given when specific comparisons are made with theory in a later section.

SUMMARY OF THE SOURCES OF ERRORS

The experimental sources of errors may be divided into two groups: (a) those influencing both the shape

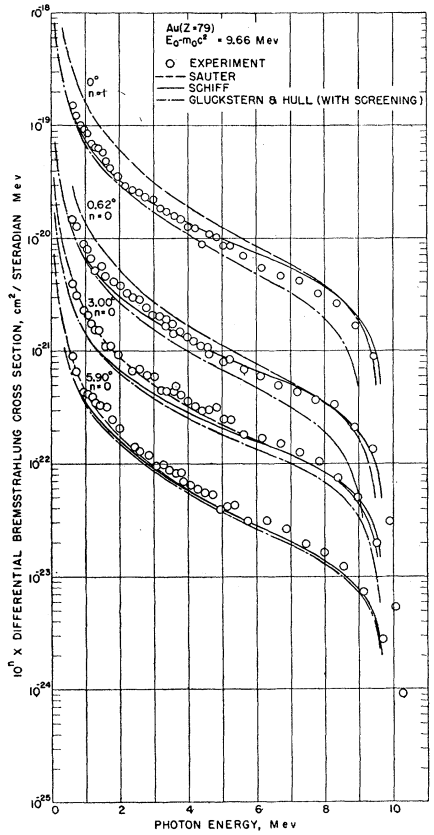

(a)

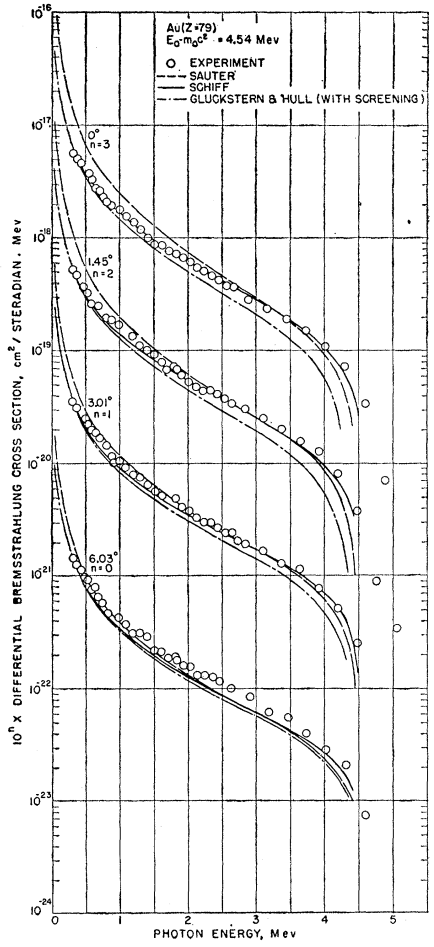

(b)

FIG. 9. Corrected experimental differential cross sections $d^2\sigma/d\Omega dk$ and theoretical cross sections according to Sauter, Gluckstern and Hull, and Schiff, respectively, for Au($Z=79$) and for electron kinetic energies (a) 9.66 Mev, (b) 4.54 Mev, and (c) 2.72 Mev.

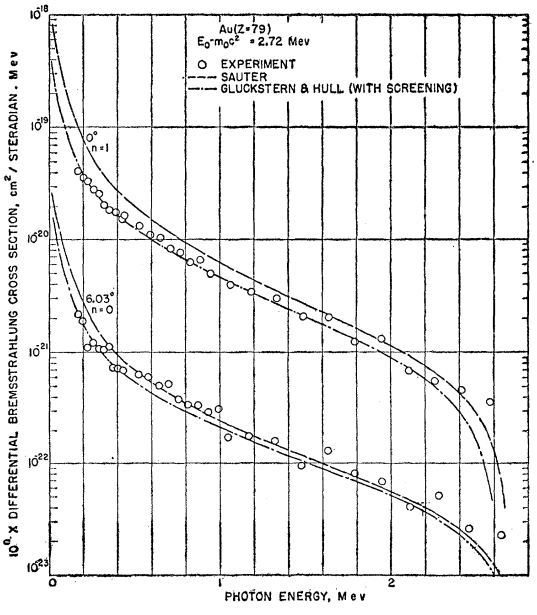

(c)

of the spectra and the absolute magnitude of the cross sections, and (b) those influencing only the latter of these quantities.

Included in group (a) are errors due to counting statistics, uncertainties in the energy calibration, uncertainties in the pile-up correction, and errors in the response function K. Furthermore, at the uppermost end of the spectrum where the intensity varied very rapidly the width of the intervals in the 56×56 matrix M caused an error which together with the counting statistics made the points above 97% of the maximum energy of the spectrum unreliable.

The errors under group (b) are larger than those of group (a). The uncertainty of $\pm0.2°$ in the determination of the angle between the electron beam and the spectrometer axis caused appreciable errors at certain

TABLE II. Percentage experimental errors for three of the measured spectra. $(E_0-m_0c^2)$ is the electron kinetic energy, k the photon energy, Z the atomic number of the nucleus, and θ the photon angle. The errors in group (a) influence both the shape of the spectra and the absolute magnitude of the cross section. Group (b) influences only the absolute magnitude.

	$(E_0-m_0c^2)$ =9.66 Mev, Z =4, θ =0.00°				$(E_0-m_0c^2)$ =4.54 Mev, Z =13, θ =6.03°				$(E_0-m_0c^2)$ =2.72 Mev, Z =79, θ =0.00°			
k Mev	0.965	3.864	7.726	9.178	0.454	1.816	3.631	4.312	0.272	1.088	2.175	2.583
$k/(E_0-m_0c^2)$	0.1	0.4	0.8	0.95	0.1	0.4	0.8	0.95	0.1	0.4	0.8	0.95
Group (a)												
Counting statistics	2.5	4.5	5.0	10.0	4.0	6.0	6.0	11.5	6.0	8.5	19.0	26.0
Energy calibration[a]	0.5	0.5	1.5	10.0	0.5	1.0	2.0	7.0	0.5	1.0	2.0	2.5
Pile-up correction[b]	0.5	1.0	1.0	2.0	0.0	0.0	0.0	0.5				
Response function	1.0	2.0	4.0	10.0	1.0	1.0	2.0	5.0	1.0	1.0	1.5	2.0
Total (rms) (a)	3.0	5.0	6.5	17.5	4.0	6.0	6.5	14.5	6.0	8.5	19.0	26.0
Group (b)												
Photon angles		3.0				6.0				0.0		
Target thickness		4.0				5.0				2.0		
Electron current		1.5				0.0				0.0		
Total (rms) (b)		5.2				8.0				2.0		

[a] Assuming ±0.5% error in energy.
[b] Assuming ±10% error in the spectrum of double pulses.

angles (9.66 Mev, 6° has the largest error of this kind). Furthermore, the finite angular interval (0.8°) involved in a spectral measurement caused an error which is important for the 0° spectra.

Another rather serious error was caused by the nonuniformity of the targets. In the case of the beryllium foil, impurities in the target were responsible for an estimated error of ±3%. The leakage current from the Faraday cage system was in most cases very small, but, for the spectra of 9.66 Mev and 0°, the change of this current could have caused an error of the order of ±2% or less.

A summary of the most important probable errors is given in Table II for three different spectra: Be, 9.66 Mev, 0°; Al, 4.54 Mev, 6°; and Au, 2.72 Mev, 0°. These spectra are representative for the respective energies. The 2.72-Mev 6° spectra have greater statistical errors than the 0° spectra because of the low intensity of the electron beam current. The statistical errors in this table are the errors estimated in the measured pulse-height distributions with the influence of the background included.[34]

COMPARISON OF THIN-TARGET RESULTS WITH THEORY

The cross sections for the emission of bremsstrahlung in the field of the nucleus, $d^2\sigma/d\Omega dk$, which are differential in the photon energy and angle, have been calculated by means of the only three available theoretical formulas and have been drawn in Figs. 7–9. These are the expressions of Sauter[8] (henceforth referred to as formula I), Gluckstern and Hull[9] (formula II), and Schiff[10] (formula III). A comparison of these predictions with the present experiments, as can be obtained from Figs. 7–9, should show the validity of the Born approximation and the screening correction, and the magnitude of the electron-electron bremsstrahlung at these energies. These should be the gross effects. Other effects, such as the effects of the finite nuclear size and multiple bremsstrahlung have been shown by Biel and Burhop[35] and by Gupta,[36] respectively, to be negligible at the angles and energies studied in this experiment.

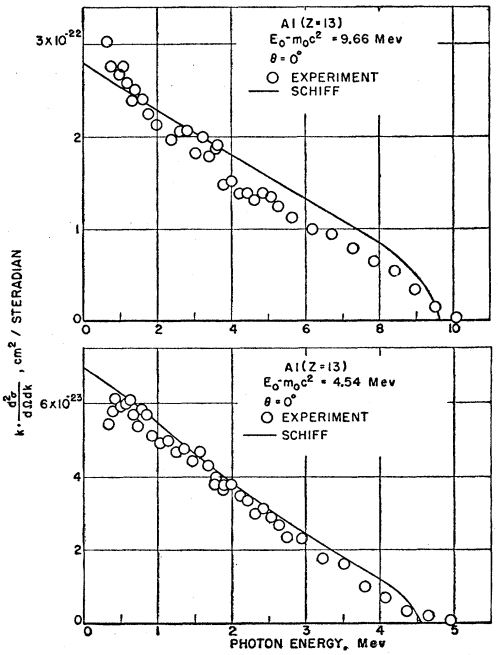

FIG. 10. Corrected experimental intensity distributions of the bremsstrahlung emitted in the forward direction and the corresponding theoretical curves for Al(Z=13) and for the electron kinetic energies of 9.66 and 4.54 Mev.

[34] The statistical errors were not evaluated by the use of the inverse matrix because of the smoothing introduced in $N(k)$ through the use of the correction factor N/P.

[35] S. J. Biel and E. H. S. Burhop, Proc. Phys. Soc. (London) **A68**, 165 (1955).
[36] S. N. Gupta, Phys. Rev. **99**, 1015 (1955).

The process of electron-electron bremsstrahlung refers to the production of an x-ray photon in the field of an electron of an atom. No theoretical calculation of $d^2\sigma/d\Omega dk$ exists for this process. However, it is known from both theory[5,37] and experiment[38] that the cross section $d\sigma/dk$ for this process integrated over photon angles is of the same order of magnitude or smaller than the cross section for bremsstrahlung in the field of a proton. Therefore, this effect can roughly be included in a prediction of $d\sigma/dk$ by replacing the Z^2 coefficient by $Z(Z+1)$. Thus, in the case of high-Z targets the experiments give almost pure nuclear bremsstrahlung. However, for a beryllium radiator, the electron-electron bremsstrahlung should contribute about 20% of the total radiation yield. The only other guide on the electron-electron bremsstrahlung is the maximum photon energy, K_0, which varies with the total energy, E_0, of the electron and the photon angle, θ, according to the expression[22]

$$K_0=m_0c^2F/(1-\cos\theta\sqrt{F}),$$

where

$$F=(E_0-m_0c^2)/(E_0+m_0c^2).$$

Table III shows some typical examples of K_0 applicable to the present experiments.

For the purpose of comparing the experimental cross sections with theory, it would be desirable to have a theoretical curve which includes an accurate screening correction and which is not based on any other restrictions on the electron and photon energies than the Born approximation. Since no adequate formula exists, the comparison will be made with the one of formulas I–III which is closest to fulfillment of these requirements in a specific photon energy range.

The three theoretical formulas (I–III) (Figs. 7–9) are different largely because of differences in the screening correction. This is obvious from a comparison of formulas I and II at large photon energies where screening becomes unimportant and the two expressions should be the same. Because of the large differences at large photon energies, formula II is considered unreliable at photon energies that are not small. Indeed, it is only at k approaching zero that Gluckstern and Hull feel their expression, corrected for screening, should be valid.

Other comparisons of the theoretical curves obtained from the formulas I–III show that formula III gives higher values than formula II for photon energies close to the high energy end of the spectra. This is most likely due to the high-energy approximations used in III, since the deviation appears to be independent of the atomic number.

Therefore, formula II should represent well a Born-approximation theory for low photon energies and formula I for high photon energies, while formula III should be reasonably good at intermediate energies

[37] J. A. Wheeler and W. E. Lamb, Phys. Rev. **55**, 858 (1939).
[38] L. Lanzl and A. O. Hanson, Phys. Rev. **83**, 959 (1951).

TABLE III. Maximum energy K_0 of the electron-electron bremsstrahlung for the electron kinetic energies $E_0-m_0c^2$ and the photon angles θ which were used in the experiments.

$E_0-m_0c^2=9.66$ Mev		$E_0-m_0c^2=4.54$ Mev		$E_0-m_0c^2=2.72$ Mev	
θ	K_0 Mev	θ	K_0 Mev	θ	K_0 Mev
0.00°	9.06	0.00°	3.83	0.00°	2.02
0.62°	9.05	1.45°	3.81	6.03°	1.97
3.00°	8.82	3.01°	3.78		
5.90°	8.25	6.03°	3.65		

where the electron and photon energies involved in the bremsstrahlung process are much larger than m_0c^2. Since formulas II and III give almost the same results at low photon energies (see Figs. 7–9), formula III will be used for $E_0=4.54$ and 9.66 Mev for all photon energies up to the point where formula I starts to give lower values than formula III. For higher photon energies, comparison will be made with formula I. Thus, the comparison theoretical curve is a composite of two theories.

A similar composite is used for the spectra produced by 2.72-Mev electrons. At this energy the extreme relativistic calculations resulting in formula III cannot be expected to give a good representation of the theory. Therefore, the comparison of the experiment with theory is made only with formulas I and II. At photon energies as low as 10% of the primary electron energy, the screening correction in formula II should be correct. Therefore, the measured cross sections are compared with this formula at $k/(E_0-m_0c^2)=0.1$. At photon energies above those for which screening is estimated to be unimportant, the experimental points are compared with formula I. These photon energies were estimated by an examination of formulas I and III for the higher electron energies.

The procedure outlined for obtaining composite theoretical cross sections should give a good representation of the Bethe and Heitler theory[5] with the screening correction. These cross sections are compared with the experiment in two parts.

In Figs. 11(a) to 11(c) the ratio of the experimental curves to the composite theoretical curves is given, with the ratio normalized to be equal to 1 at $k/(E_0-m_0c^2)=0.5$. After normalizing the ratios, the shapes of the experimental curves obtained for one target and one electron energy at the different photon angles were very similar in shape. Therefore, the ratio curves at the different angles were averaged and plotted as one of the curves in Figs. 11(a) to 11(c). The experimental errors calculated for single points on the experimental curves of Figs. 7–9 are drawn on Figs. 11(a) to 11(f). Since each of the points in Figs. 11(a) to 11(c), in the energy range below $k/(E_0-m_0c^2)=0.6$, represents several experimental points, the errors in the normalized ratios should be somewhat smaller than the estimated errors shown on the figures.

The normalized ratio curves of Figs. 11(a) to 11(b)

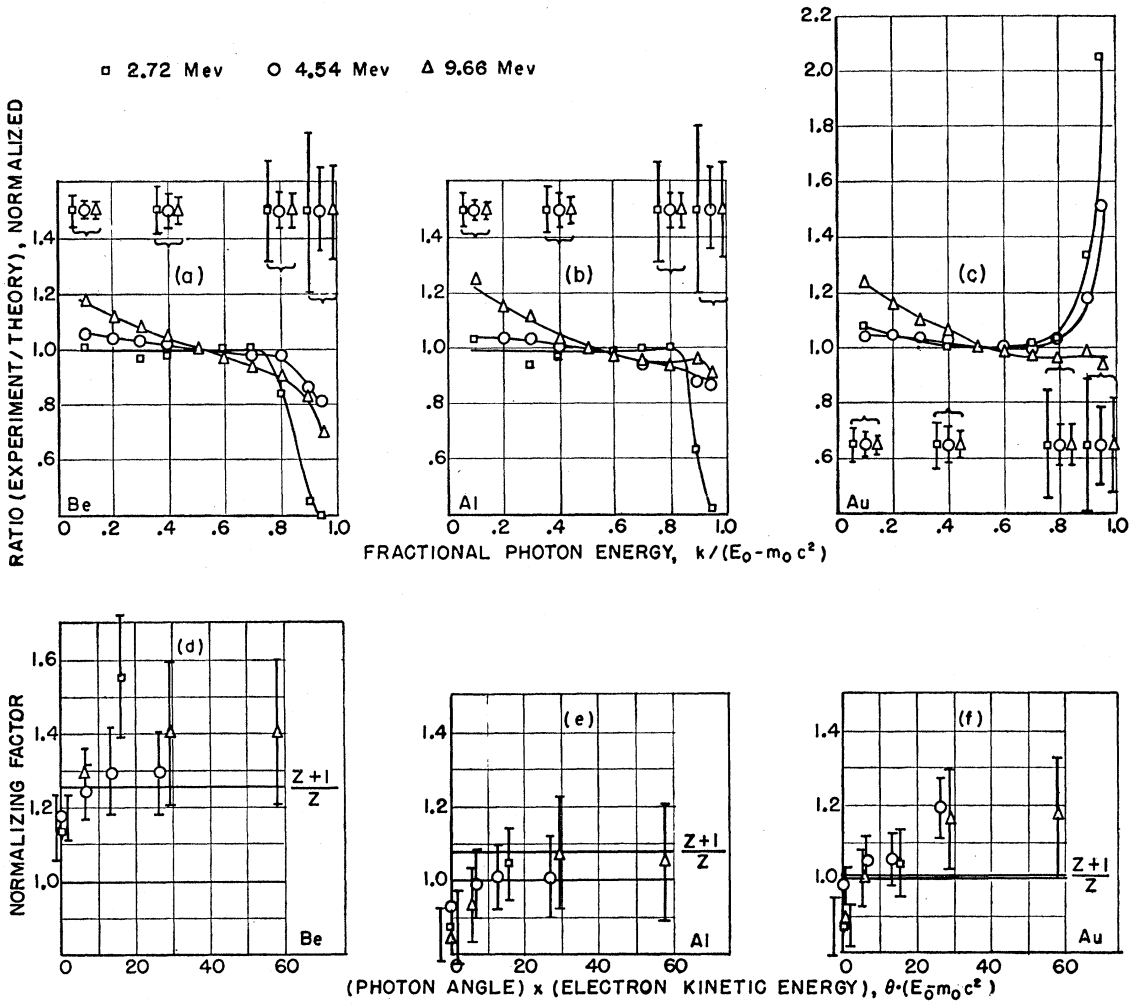

FIG. 11. Comparison between the experimental and the theoretical cross sections for Be, Al, and Au. For the 9.66- and 4.54-Mev spectra the theory is represented by Schiff's formula for $k/(E_0-m_0c^2)$ less than approximately 0.8 and by Sauter's formula for higher photon energies. For the 2.72-Mev spectra Sauter's formula is used for all $k/(E_0-m_0c^2)$ except 0.1 where Gluckstern and Hull's formula including screening is used. In (a)–(c) the ordinate is the ratio between experiment and normalized theory and the abscissa is the fractional photon energy. In (d)–(f) the ordinate is the normalizing factor used in (a)–(c) at $k/(E_0-m_0c^2)=0.5$. The abscissa scale is the photon angle times the electron kinetic energy.

show that below a fractional photon energy of 0.8, the 9.66-Mev spectra for the three targets studied are steeper than the theoretical spectra represented by formula III (Schiff).[39] The 4.54-Mev and the 2.72-Mev spectra agree with theory within the experimental errors for fractional photon energies less than 0.8.

The ratio between experiment and normalized theory does not change appreciably at a given electron energy with either the atomic number of the target or the photon angle below $k/(E_0-m_0c^2)=0.8$. Thus, there can be little difference in shape between the electron-nuclear and the electron-electron bremsstrahlung spectra, since electron-electron processes would have affected the shapes of the Be spectra but not the Au spectra.

[39] Similar indications were obtained for an electron kinetic energy of 11 Mev by Motz, Miller, and Wyckoff in reference 14.

The great differences between experiment and theory occur for fractional photon energies larger than 0.8. Theory is here represented by formula I (Sauter) for all the spectra. For the low-Z materials (Be and Al), the experimental points lie below theory in 90% of the cases. This fact can be explained to some extent by the high-energy cutoff of the electron-electron bremsstrahlung (Table III). However, the experimental errors are too large here to permit any definite conclusions. For the high-Z radiator (Au), the experimental points lie without doubt above theory for the 4.54-Mev spectra and still more so for 2.72 Mev. This effect is ascribed to the nonvalidity of the Born approximation for large atomic numbers and for low outgoing electron velocities. It is interesting to see that the experiments at 9.66 Mev agree with theory for fractional energies as high as 0.95. This is in agreement with other experi-

ments as described in the introduction, which indicate that the Born approximation theory should give too large values for the bremsstrahlung cross section integrated over photon angle and energy for low primary electron energies and too small values for high electron energies with the transition energy close to 5 Mev.

It should be pointed out that the Born approximation is supposed to be valid if $2\pi Z/137\beta \ll 1$ both for the incoming and the outgoing electron. This requirement is never fulfilled for $Z=79$. However, it implies that points in the different spectra corresponding to the same velocity of the outgoing electron should be intercompared. In this respect $k/(E_0-m_0c^2)=0.95$ in the 9.66-Mev spectrum corresponds to $k/(E_0-m_0c^2)=0.89$ in the 4.54-Mev spectrum and to $k/(E_0-m_0c^2)=0.82$ in the 2.72-Mev spectrum. None of these points shows any definite deviation from theory.

In Figs. 11(d) to 11(f) an attempt is made to compare the absolute yield of bremsstrahlung with theory. The normalizing factor used for the comparison of the spectral shapes, that is the ratio between experiment and theory at $k/(E_0-m_0c^2)=0.5$, is plotted as a function of the product of the photon angle and the electron kinetic energy in order to allow the data for different electron energies to be intercompared on one graph. In the case of the 4.54-Mev and the 2.72-Mev spectra, where the experimental and theoretical shapes agree, this factor, of course, represents very well the ratio between the measured and the theoretical value of the total energy radiated in a certain direction. Because of the shape differences [see Figs. 11(a) to 11(c)], this ratio is of the order of 10% larger than the normalizing factor for the 9.66-Mev spectra. However, this difference is unimportant because the experimental errors for these spectra are larger than 10% for all angles except 0°. The errors result from the great influence of the small error in the measurement of the photon angle θ. This error appears mainly in the determination of the 0° direction and should thus give almost the same errors for all the three elements studied.

Because of the magnitude of the errors it is fairly difficult to conclude anything about the angular distribution of the bremsstrahlung. However, the variation of the normalizing factor with angle in Figs. 11(d) to 11(f) is similar for all the three values of Z and thus should not be due to a difference between the angular distribution of the nuclear and the electron-electron bremsstrahlung. The variation implies that the theory gives somewhat too large values at $\theta=0°$ and somewhat too small values at other angles studied.

As was pointed out above, the measured cross sections integrated over photon angles should be approximately $(Z+1)/Z$ larger than theory because of the effect of electron-electron bremsstrahlung. The experimental results support this assumption, since Figs. 11(d) to 11(f) show that the Be normalizing factor is always about 25% larger than the factors for Al and Au at corresponding angles. The factors also cluster around the $(Z+1)/Z$ line drawn for comparison on the figures, although the experimental errors are large. The fact that all of the Al points lie below the $(Z+1)/Z$ line, while the Be and Au points for angles different than 0° lie above the line, is most likely due to the error in the target thickness which is larger for Al than for the other two elements.

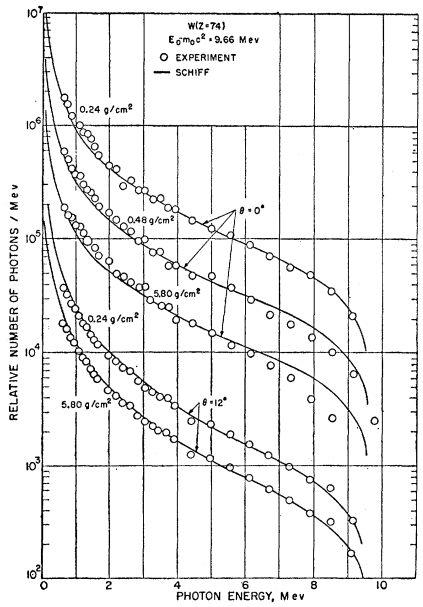

FIG. 12. Corrected experimental photon spectra for three thick W targets for an electron kinetic energy of 9.66 Mev at the photon angles of 0° and 12°. The solid line represents Schiff's thin-target spectrum normalized to the experimental points at $k/(E_0-m_0c^2)=0.5$.

In a comparison of the present measurements with the bremsstrahlung cross-section measurements by Motz for 0.5- and 1.0-Mev electrons, certain of his findings are confirmed. For example, he concluded that in the case of high-Z ($=79$) nuclei, the departure from the theoretical curves increases as (a) the photon angle of emission θ increases, (b) the photon energy increases, and (c) the initial electron kinetic energy decreases. The trends (b) and (c) are in very good agreement with the present results. The point (a), however, is not so obvious at the higher electron energies and the smaller angles used in the present experiment.

The experimental procedure used in the present experiment for primary electron energies between 2.5 and 10 Mev probably could be extended to an energy of 20 Mev. Above this energy the difficulties in determining the response function of the spectrometer increase. Also with increasing electron energy, the deviations between experiment and theory are in general assumed to decrease. Therefore, an experiment with higher accuracy would be required to determine these deviations. One difficulty that increases with energy is the determination of the photon angle. The

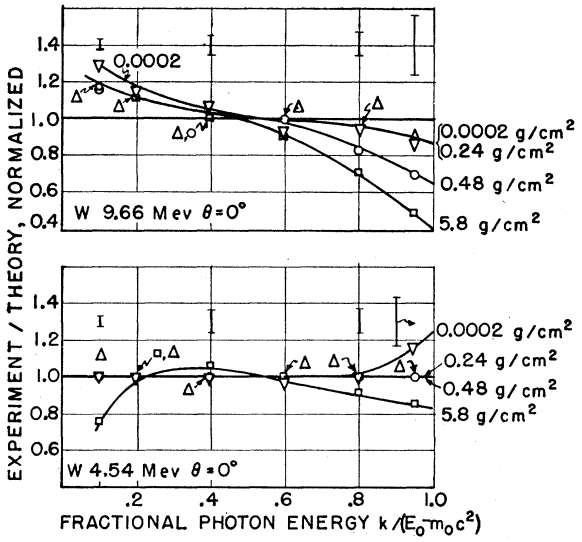

FIG. 13. Comparison between the experimental thick-target W spectra and Schiff's thin-target spectra normalized to the experiment at $k/(E_0-m_0c^2)=0.5$. The curves labeled 0.0002 g/cm² are data for gold obtained from Fig. 11.

accuracy in this quantity would have to be increased directly as the energy, and the spread of the electrons in the beam and the angular aperture of the spectrometer would have to be decreased in the same proportion. Another problem connected with higher energies would be the serious background of neutrons caused by photoneutron reactions in the Faraday cage, defining apertures, and shielding walls.

The most needed spectrum characteristic at energies above 10 Mev is the shape of the high photon-energy part of the spectrum. Unfortunately, the technique used in the present experiment would be unsuitable for defining the shapes for fractional photon energies larger than 0.95. All of the experimental errors are considerably larger in this energy range than in the rest of the spectrum.

COMPARISON OF THICK-TARGET RESULTS WITH THEORY

In the experiments with the thick tungsten targets, the number of electrons passing through the target during a spectrum determination was not measured. Therefore, only the shapes of the spectra were obtained. Figure 12 shows the experimental results and the theoretical thin-target cross sections according to Schiff's formula for an electron kinetic energy of 9.66 Mev and x-ray photon angles of 0° and 12°. The data for an energy of 4.54 Mev have been omitted. The theoretical curves were normalized to the experimental results at $k/(E_0-m_0c^2)=0.5$. Figure 13 shows the ratios between the experimental and the normalized theoretical thin-target curves for an electron energy of 9.66 Mev and 4.54 Mev. As was expected, the deviation from the thin-target theory increases with target thickness because of the energy loss of the electrons in the thick targets. Also the self-absorption of the x-rays in the targets tends to reduce the experimental values for low photon energies and increasing target thicknesses.

ACKNOWLEDGMENTS

The authors are very grateful to Dr. M. Danos for many helpful discussions and suggestions throughout the course of this investigation. Thanks are also due to Dr. J. W. Motz for interesting discussions, to Dr. E. G. Fuller and Dr. B. Petree for their help with the electron beam removal equipment, to Dr. Morris Newman for inverting the response function matrix, and to Miss Irene Stegun for evaluating the various theoretical expressions.

One of us, Nils Starfelt, wishes to express his gratitude to the Betatron Section of the National Bureau of Standards for the opportunity of working in its laboratories and to the two Swedish organizations, "Statens Naturvetenskapliga Forskningsråd" and "Riksföreningen för Kräftsjukdomarnas Bekämpande," for financial grants.